

## Surface layer temperature inversion in the Bay of Bengal

Pankajakshan Thadathil, V.V. Gopalakrishna, P.M. Muraleedharan, G.V. Reddy and Nilesh Araligidad  
National Institute of Oceanography, Dona Paula, Goa 403 004, India  
Email:pankaj@darya.nio.org

### Abstract

Hydrographic and XBT data archived in the Indian Oceanographic Data Centre (IODC) are used to understand the process of temperature inversions occurring in the Bay of Bengal. The following aspects of the inversions are addressed: i) annual distribution of the layer thickness, layer gradient, starting depth and their inter-annual variability, ii) static stability of the layer and iii) generating mechanism/s. It is seen that organized inversions in the bay occur during winter (from November to February) and the occurrence is mainly in the coastal/offshore waters. By January, the occurrence region shifts from the coastal waters of western bay towards the central and eastern region (Andaman Sea). Inversions of large temperature gradient ( $\Delta T$ ) of the order of 1.6–2.4°C and thin layer thickness ( $\Delta D$ ) (10–20 m) are located adjacent to the three major fresh water zones (Krishna, Godavari; Ganges, Brahmaputra and Irrawady).

Inter-annual variability of the inversion occurring in the bay is examined utilizing XBT data collected along Andaman–Calcutta section during winter months of different years. Inversion layers with strong  $\Delta T$  and  $\Delta D$  are present in all the years with significant inter-annual variability. The vertical stability in temperature inversion layers are addressed based on the  $\Delta S - \Delta T$  ( $\Delta S$  is the salinity gradient corresponding to  $\Delta D$ ) relationships derived from inversion profiles. The  $\Delta S - \Delta T$  plot revealed the existence of two clusters with  $\Delta T$  values  $> 2^\circ\text{C}$  and  $< 2^\circ\text{C}$  located north and south of  $18^\circ\text{N}$ , respectively. While the stability of inversions north of  $18^\circ\text{N}$  is  $3600 \times 10^{-8} \text{ m}^{-1}$ , south of  $18^\circ\text{N}$ , it is  $3000 \times 10^{-8} \text{ m}^{-1}$ .

The role of net surface heat flux in generating the observed inversions are examined from the climatological monthly estimates of the same derived from ISCCP (International Satellite Cloud Climatology Program), SRB (Surface Radiation Budget) radiational and COADS turbulent fluxes. In November and December, the surface heat loss in the coastal region cools the surface waters and because of the high stratification (caused by fresh water) the cool surface layer stay stagnated in the first few meters favoring the formation of temperature inversion. The organized inversions occurring in the central and northeastern bay (north of Andaman Sea) in January and February appears to be generated due to the horizontal advection. Since the net surface heat flux shows heat gain in this region, the organised inversions in this region appears to be generated by the cold fresher water advection (from the head of the bay and Irrawadi basin) over the remnant of the warm saline water in this region advected by the southwest monsoon drift current.

### 1. Introduction

The stability of the oceanic surface layer depends largely on temperature compared to the salinity. This results in the characteristic vertical distribution of temperature; a surface warmer mixed layer and subsequent colder sub-surface layers. However, in regions where the surface salinity is diluted with fresh water influx, salinity plays an equal or dominant role in controlling the stability of the layer. In such cases, the normal distribution of temperature could be altered to form a sub-surface warm layer (inversion layer), sandwiched between colder waters above and below. Here, the salinity compensates the stability loss caused by the temperature inversion. In the Bay of Bengal, the winter cooling caused by surface heat loss and the resulting convective mixing is confined to a very thin surface layer. The large river run-off and excess precipitation over evaporation during summer monsoon distribute fresher water in the bay. Thus the barrier layer set in

during summer restrict the convective mixing caused by surface cooling during winter to a thin surface layer and set the conditions favorable for the formation of temperature inversions. Temperature inversions also occur in frontal zones where the warm water meets colder water, such as the Kuroshio and Oyashio (Nakata 1979). Though such strong thermal fronts are not present in the Bay of Bengal, temperature inversions were reported in the coastal waters of western and northern Bay of Bengal during winter (Panakala Rao and Sastry 1981, Rao et al. 1983, Prabhakara Rao et al. 1987, Shetye et al. 1996, Suryanarayana et al. 1995). In this study, effort is made to understand the process of temperature inversions occurring in the bay by using the hydrographic and XBT data archived in the Indian Oceanographic Data Centre (IODC). The following aspects of the inversions are addressed:

(i) annual distribution of the layer thickness, layer gradient, starting depth and their inter-annual variability,

- (ii) static stability of the layer and
- (iii) generating mechanism/s.

**2. Annual distribution**

In order to identify the occurrence region of temperature inversion in the bay, all the available temperature profiles are sorted out for each 1° x 1° bin. The total number of profiles, available in each one degree bin on monthly basis, are represented in three ranges; less than 5, between 5 and 10, and greater than 10. Then the number of inversion profiles existing in each one degree bin are represented as the ratio between num-

ber of profiles with inversions and total profiles (filled portions of the circles represent the occurrence ratio) in each one degree bin. The circles are shown at center of each 1° x 1° bin. Fig. 1 represents the monthly distribution of the occurrence of temperature inversions observed in the bay. In this study, we have considered only those temperature profiles where the inversions are greater than 0.5°C. It is seen from Fig. 1 that organized inversions in the bay occur during winter (from November to February). Random occurrence of inversions are visible during March–April and appears to be the remnant of the organized inversions occurred during winter. Isolated inversions are also visible in the

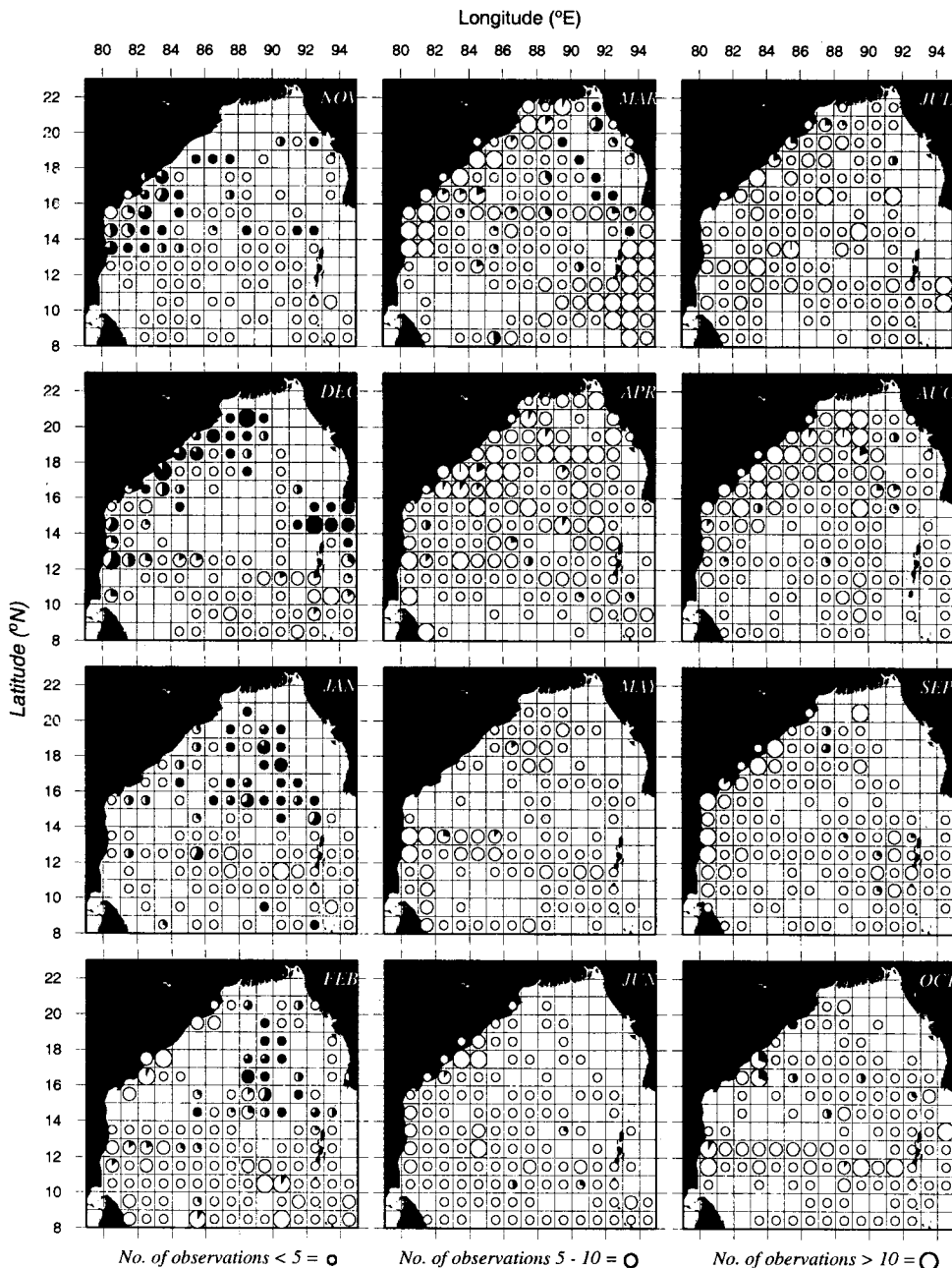


Fig. 1. Monthly distribution of occurrence of temperature inversion in the Bay of Bengal.

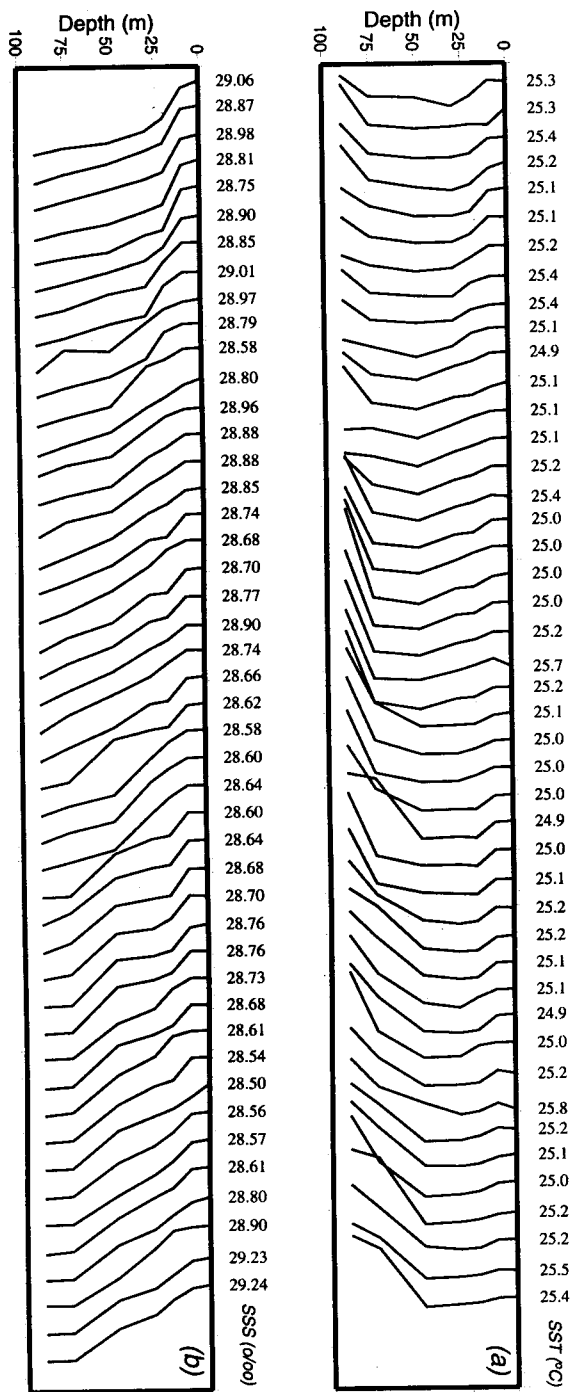


Fig. 2(a). 3 hourly time series temperature profiles at 17°N 83°E for the period 21-27 December 1983, (b) 3 hourly time series salinity profiles at 17°N 83°E for the same period.

summer monsoon season. Since large-scale organized inversions are visible only in winter, the subsequent discussion is mainly focused on winter inversions.

In November and December, the occurrence is mainly in the coastal / offshore waters of the bay. However, its presence in the coastal waters of north-eastern bay is not known as there are no observations from this

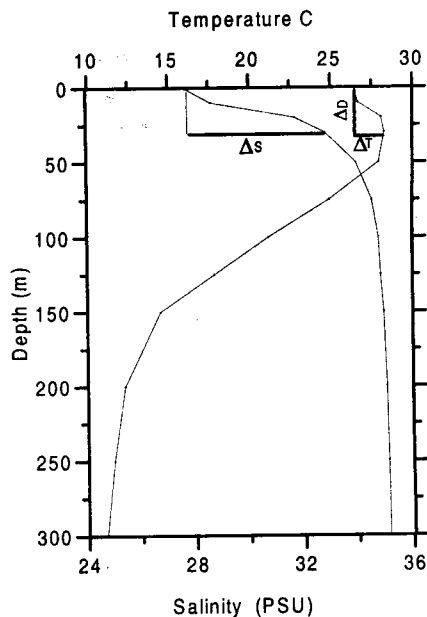


Fig. 3. Temperature and salinity profiles indicating inversion layer characteristics.

region. By January, the occurrence region shifts from the coastal waters of western bay towards the central and eastern region (Andaman Sea). Such a shift is more obvious in the month of February, when there are enough observations in the coastal grids without inversions.

### 3. General characteristics of the inversion layer

Three hourly observations of temperature and salinity profiles collected from a stationary position (17° N, 83° E) for the period 21-27 December, 1983 are presented in Fig. 2a and fig.2b respectively. Temperature inversions are persistent throughout the observation period without showing any indication of either the growing or the decaying stage. No significant changes are noticed in layer thickness and its gradient. It is seen from Fig. 3b that the inversion layers are occurring within the halocline. The general characteristics: layer thickness ( $\Delta D$ ), layer gradient ( $\Delta T$ ), starting depth ( $D_s$ ) and the salinity gradient ( $\Delta S$ ) equivalent to  $\Delta D$  do not show any significant diurnal variability. Typical temperature and salinity profiles representing the above characteristics are illustrated in Fig. 3.

Distributions of  $\Delta T$ ,  $\Delta D$  and  $D_s$  are given in Figs. 4a - 4c, respectively. Inversions of large temperature gradient of the order of 1.6-2.4 °C (Fig. 4a) are located adjacent to the three major fresh water zones (Krishna, Godavari, Ganges, Brahmaputra and Irrawadi). Inversion layer thickness (Fig. 4b) is thinner (10-20 m) in the coastal/offshore waters (where large  $\Delta T$ s are observed) compared to open ocean, where  $\Delta D$  varied be-

tween 40 and 50 m. The starting depth of inversions ( $D_s$ ) follows nearly the same distribution pattern as that of layer thickness, with smaller values of  $D_s$  (10 - 20 m) in the coastal waters and greater  $D_s$  (30 - 40 m) in the open ocean region south of 16°N (Fig. 4c).

#### 4. Inter-annual variability

In order to examine the inter-annual variability of the inversion occurring in the bay, XBT data collected along Andaman-Calcutta section during winter months of different years (1994, 1995, 1997, 1998, and 2000) have been considered. Snap-shot thermal sections for these years are presented in Fig. 5. Inversion zones in each of the sections are demarcated by area surrounded by thick line. Inversion layers with strong  $\Delta T$  and  $\Delta D$  are present in all the years with significant inter-annual variability. In general, inversions are more prominent in the Andaman Sea region. In January 1997, the entire section (about 600 Km) shows a continuous inversion layer with large layer gradient and thickness.

#### 5. Vertical stability

The vertical stability in temperature inversion layers in the ocean depends upon the degree to which the increase in temperature with depth is compensated by the rise in salinity. Federov (1978) examined the  $\Delta S - \Delta T$  relationship of temperature inversion layers in the Atlantic Ocean and the Sea of Okhotsk and reported that the  $\Delta S - \Delta T$  relationships serve as a measure of their vertical stability. Neglecting the adiabatic temperature change in the surface layer, the static stability ( $E$ ) of the inversion layer can be expressed as

$$E = \frac{-1}{\rho} \left[ \left( \frac{\partial \rho}{\partial T} \right) \left( \frac{\partial T}{\partial Z} \right) + \left( \frac{\partial \rho}{\partial S} \right) \left( \frac{\partial S}{\partial Z} \right) \right] m^{-1} \quad (1)$$

Where  $\rho$ ,  $S$ ,  $T$  and  $Z$  are density, salinity, temperature and the vertical coordinate, respectively. Considering

$\frac{-1}{\rho} \left( \frac{\partial \rho}{\partial T} \right)$ , the coefficient of thermal expansion ( $\alpha$ ) and

$\frac{1}{\rho} \left( \frac{\partial \rho}{\partial S} \right)$ , the coefficient of saline contraction ( $\beta$ ) are constants, Equ. 1 can be simplified as

$$E = \alpha \left( \frac{\partial T}{\partial Z} \right) + \beta \left( \frac{\partial S}{\partial Z} \right) m^{-1} \quad (2)$$

Since the stability may vary substantially within the inversion layer, a better estimate would be the mean

stability defined as  $E = \left( \frac{1}{h} \right) \int E(z) dz > 0$ , where

$h = \Delta D$ . Considering this mean stability, Equ. 2 could be re-written as

$$\Delta S = \left( \frac{\alpha}{\beta} \right) \Delta T + E \left( \frac{h}{\beta} \right) \quad (3)$$

Equ. 3 represents the linear  $\Delta S - \Delta T$  relationship of inversion layers suggested by Federov (1978). The  $\Delta S - \Delta T$  plot revealed the existence of two clusters with  $\Delta T$  values  $> 2^\circ\text{C}$  and  $< 2^\circ\text{C}$  located north and south of 18°N, respectively. The large  $\Delta T$  values north of 18°N can be attributed to the lowest temperatures, ( $< 26^\circ\text{C}$ ), present in this region during winter (Fig. 7 – right panels). The corresponding regression equations are:

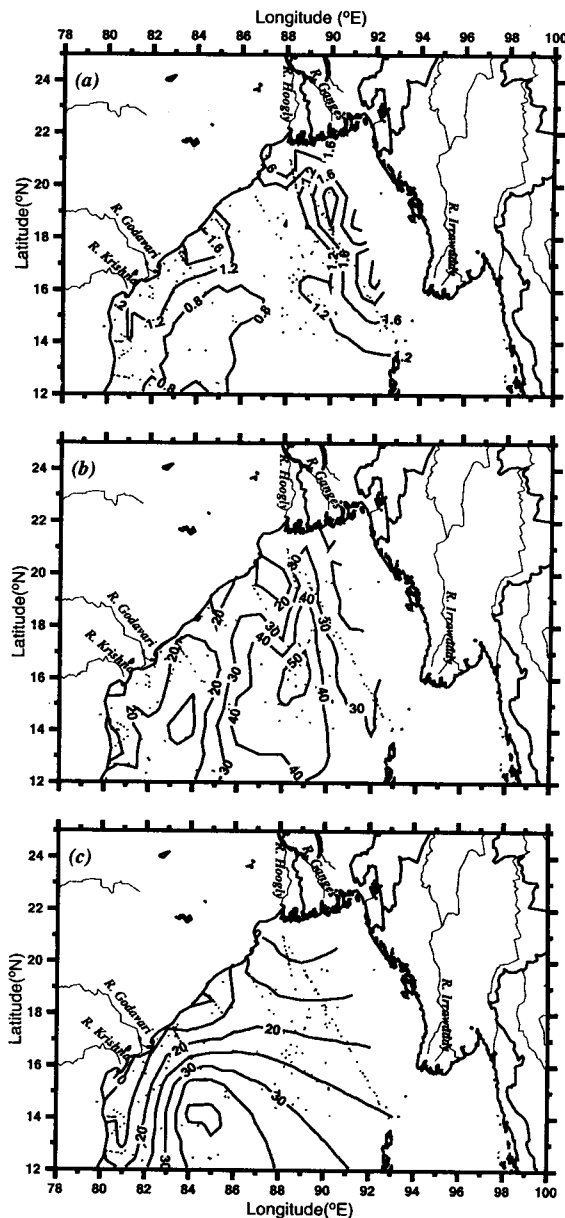


Fig. 4(a). Distribution of inversion layer temperature gradient ( $\Delta T$ ) for winter, (b) Distribution of inversion layer thickness ( $\Delta D$ ) for winter, (c) Distribution of inversion layer salinity gradient ( $\Delta S$ ) for winter.

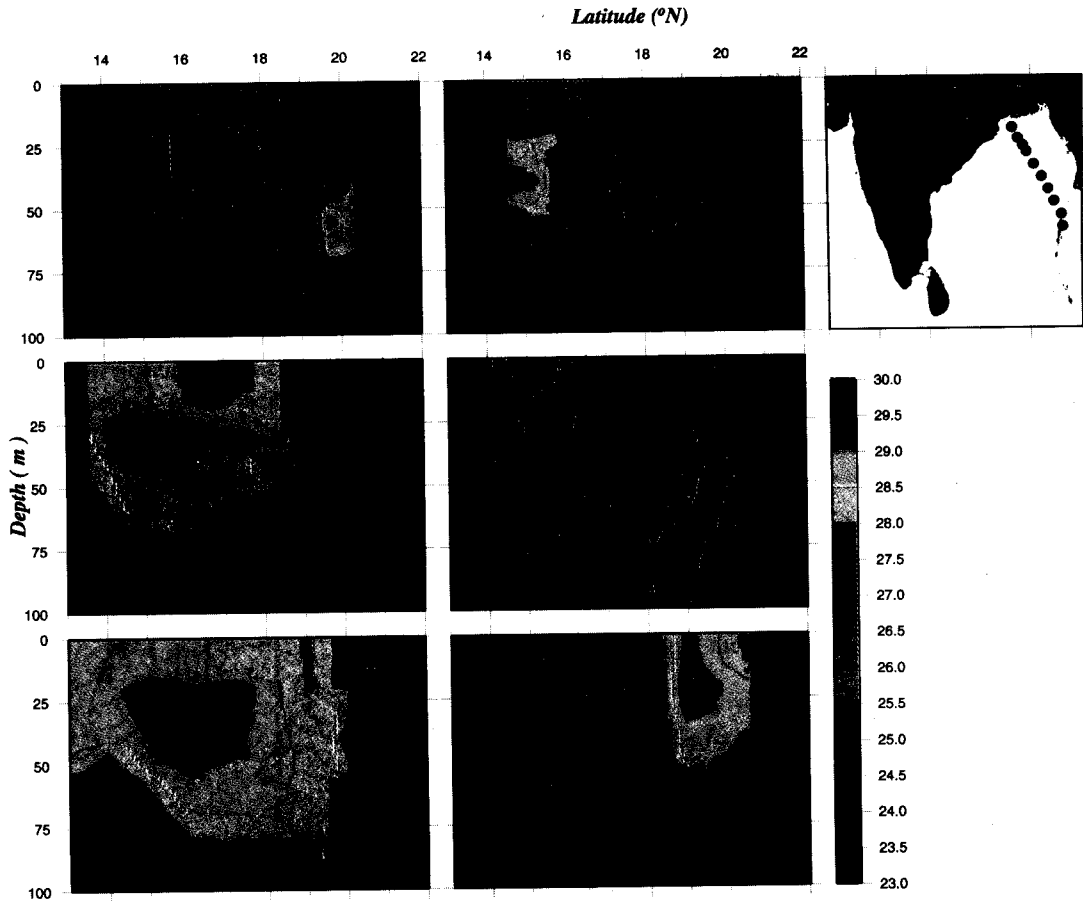


Fig. 5. Snap-shot thermal sections along Andamans-Calcutta XBT track for winter season of different years.

$$\Delta S = 0.82\Delta T \quad \text{North of } 18^\circ N \quad (4)$$

$$\Delta S = \Delta T + 1.2 \quad \text{South of } 18^\circ N \quad (5)$$

The correlation coefficients are 0.6 and 0.8 for eqn. 4 and 5, respectively and are significant at 95% confidence level. The scatter is more for  $\Delta S - \Delta T$  relation south of  $18^\circ N$  and to some extent, the observed scatter could be attributed to the depth resolution at which temperature and salinity data were available. When the depth resolution of the temperature data is  $> 5$  m, it is difficult to detect and measure the actual extreme temperature and salinity values in the inversion layer, and hence to obtain true values of  $\Delta S$  and  $\Delta T$ . CTD data set of 1 m (or less) depth resolution can minimize such scatters. In this study, we used CTD data at 5 m intervals and hydrocast (Nansen) data at standard depths.

In the northern bay, where the temperature inversion forms against the background of a sharp increase in salinity with depth (strong halocline), there exists no natural restrictions for  $\Delta T$  and the  $\Delta S - \Delta T$  relation follows the form

$$\Delta S = \left( \frac{\alpha}{\beta} \right) \left( \frac{\Delta T}{(k-1)} \right) \quad (6)$$

$\Delta S = \Delta S_0 + k\Delta S$ , where  $\Delta S_0$  represents the salinity gradient necessary for neutral stability.

$$\Delta S = \frac{\Delta S_0}{(1-k)} \quad (7)$$

From equation 6, the coefficient 'k' is obtained as 0.6. This indicates that the vertical salinity gradient  $\Delta S$  in the northern bay is several times larger than the salinity gradient necessary  $\Delta S_0$  for balancing the decline in density with depth because of the temperature inversion. The excess salinity gradient could be worked out as follows:

In the case of northern bay,  $\Delta S_0 = 2.5 \Delta S_0$  and the stability,  $E = \frac{\beta k \Delta S}{h} = 3600 \times 10^{-8} m^{-1}$ . For the inversions south of  $18^\circ N$ , the stability of the inversion layer is obtained by comparing the intercepts of eq. 5 with eq. 3.

$$\frac{Eh}{\beta} = 1.2, \quad E = \frac{1.2\beta}{h} = 3000 \times 10^{-8} m^{-1}$$

In this case, the intercept 1.2 indicates the salinity gradient existing more than that required to compensate the stability loss due to the inversion layer.

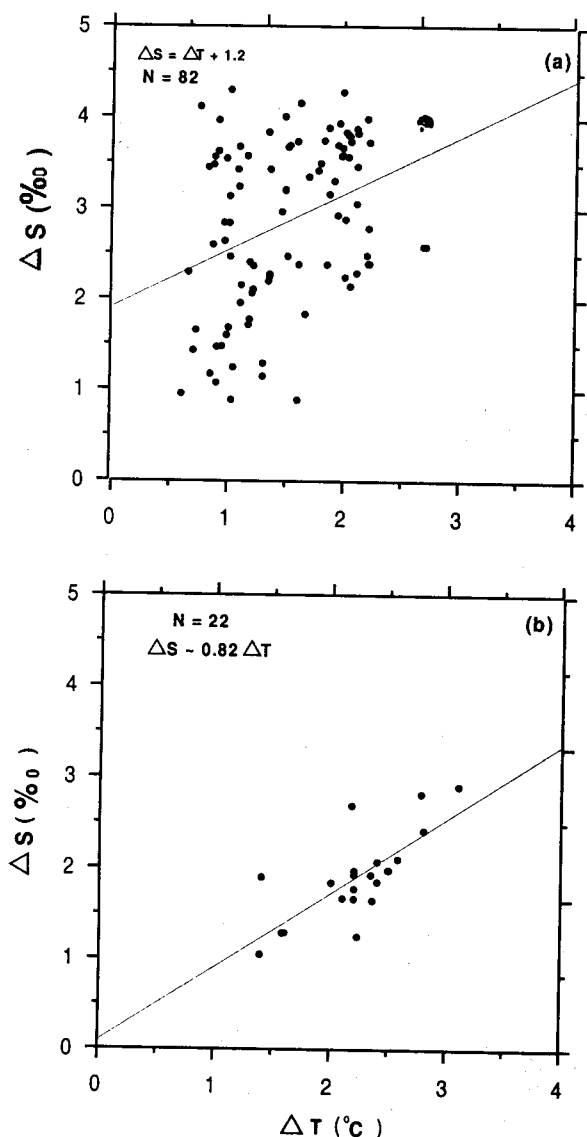


Fig. 6(a). Scatter plot between  $\Delta S$  and  $\Delta T$  for south of  $18^{\circ}N$ ,  
(b) Scatter plot between  $\Delta S$  and  $\Delta T$  for north of  $18^{\circ}N$ .

## 6. Causative factors

Mechanisms responsible for temperature inversions originate either from the atmosphere or from the ocean interior. Since the observed inversions in the bay are confined to the upper few tens of meters, an active regime of surface forcings, we examine the role of following generating mechanisms:

- (i) net surface heat loss and associated surface cooling.
- (ii) the advection of cold-fresher water over warm-saline water.

### 6.1 Net surface heat loss

Using the International Satellite Cloud Climatology Project (ISCCP) C1 data, Darnell et al. (1992) computed the seasonal estimates of Surface Radiation

Budget (SRB) on a global scale. This data set, known as the Langley short and longwave surface radiation budget data set, is available in CD as well as on NASA's web-site. In this study, we make use of the short and long wave data for the Bay of Bengal for the period 1984-1990 for deriving the climatological monthly means of the net heat flux at the sea surface. Sensible and latent heat fluxes are derived from COADS surface meteorological parameters for the same period of the SRB data set and compute the climatological monthly means. While the spatial resolution of the COADS data set is  $2^{\circ} \times 2^{\circ}$ , for the SRB data set, it is  $2.5^{\circ} \times 2.5^{\circ}$ . The SRB data sets are spatially interpolated (Krigging method) and reduced to the same spatial resolution of that of COADS. Since the SRB radiation budget is based on the radiative transfer model and does not involve any bulk parameterisation, the expected accuracy for both short and long wave budget is of the order of  $10 \text{ Wm}^{-2}$ . In the case of bulk method using cloud coverage, the error is much higher. By combining the satellite observed SRB data with COADS turbulent fluxes, we expect better estimates of the net surface heat flux available for the bay. Climatological monthly means of the net surface heat flux, derived as above, for the bay during the winter season (November–February) are given in Fig.7, left panels. The maximum heat loss ( $60 - 80 \text{ Wm}^{-2}$ ) in the bay occurs during November and December and these zones are confined to the coastal waters of the western and northern bay with an offshore decreasing trend. While the heat flux contours in November run parallel to the east coast, in December, the contours bulge offshore at the central east coast towards the central bay. In January and February, there is a marked change in the distribution. Except very limited zones in the north-east and the extreme north, the entire bay shows heat gain, with the maximum heat gain zones located at the central east coast of India and the south eastern bay.

While the occurrence of organised inversions in November and December is seen in the coastal waters of the western bay, by January the occurrence zones shift away from the coastal waters to the central and eastern bay. In November and December, the surface heat loss in the coastal region cools the surface waters and because of the high stratification (caused by fresh water) the cool surface layer stay stagnated in the first few meters favoring the formation of temperature inversion. By January and February though the net surface heat flux shows gain for this region, the cold water is advected to south by the east India coastal current (Shetye et al. 1995).

### 6.2 Horizontal advection

The organized inversions occurring in the central and northeastern bay (north of Andaman Sea) in January

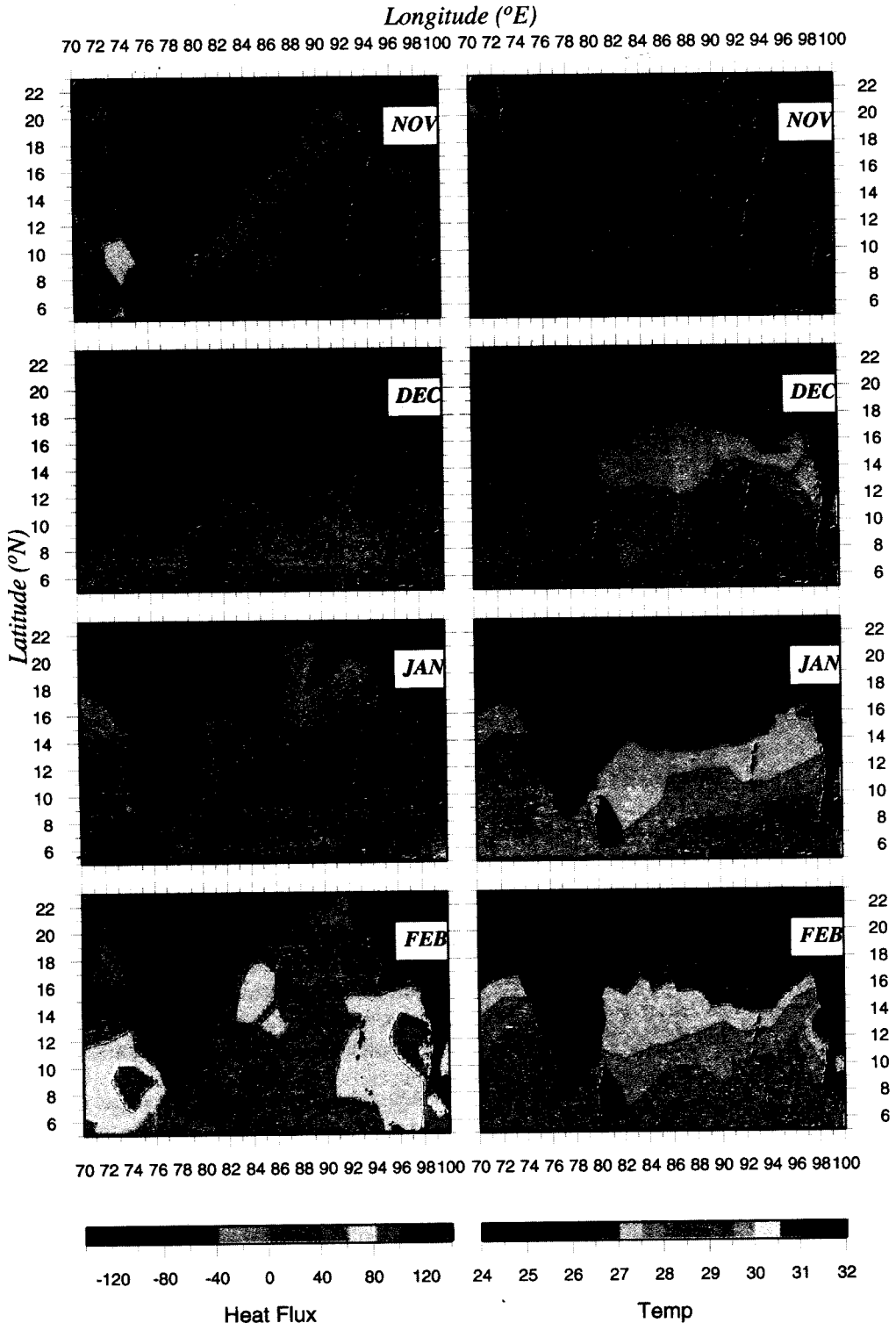


Fig. 7. Distribution of mean monthly net surface heat flux ( $w/m^2$ ) left panels and SST right panels during winter.

and February appears to have a different generating mechanism other than the surface heat loss and associated cooling. The observed inversions in this region could be generated due to the horizontal advection. Murthy et al. (1992) observed that during the summer monsoon period monsoon drift current advects a warm

and saline water mass north eastward of the bay up to  $14^\circ N$  at the depth limits of 50–100 m. Suryanarayana et al. (1993) reported the presence of this warm saline water in the north eastern bay at a depth of 50 m in the early winter. Fig. 8a-d represent the surface current vectors extracted from the drifter data for the winter

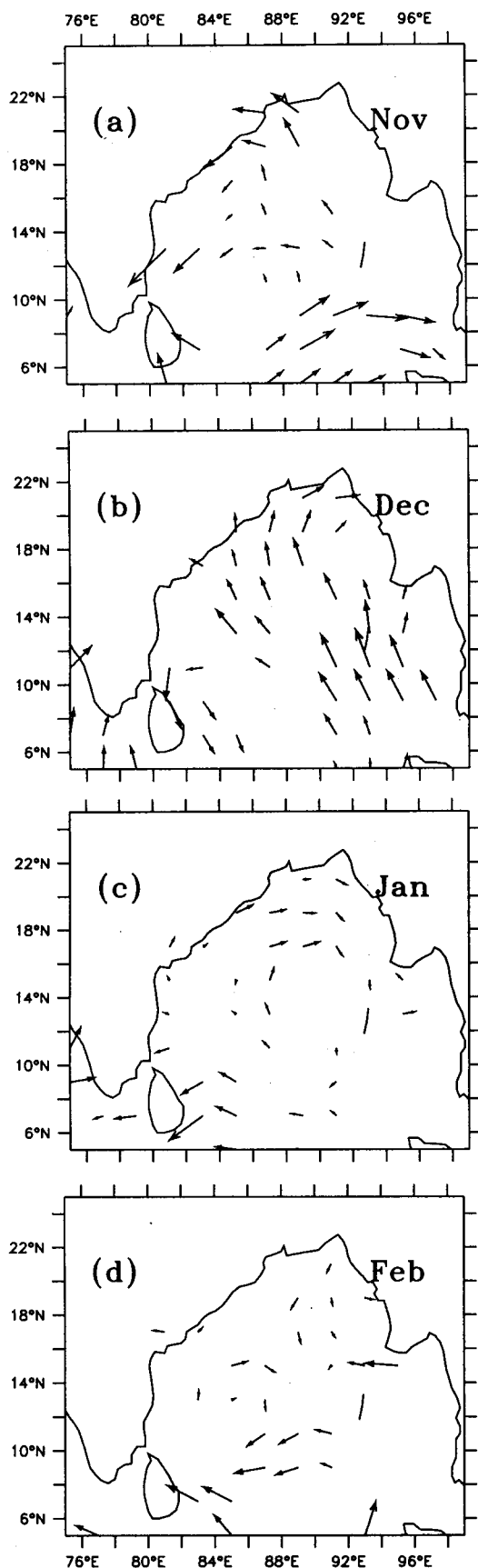


Fig. 8. Mean monthly velocity vectors estimated from drifter data (after Shenoi et al., 1999).

season. Cold and fresh water from the head of the bay and Irrawaddy basin drift southward and westward and eventually advect over the remnant of the warm saline water in this region advected by the southwest monsoon drift current. Since the net surface heat flux shows heat gain in this region, the organized inversions in this region appear to be generated by the cold fresher water advected (from the head of the bay and Irrawaddy basin) over the warm saline water mass existing in this region at about 50 m depth.

#### Acknowledgements

The authors thank Dr. V.S.N. Murty, National Institute of Oceanography for his valuable suggestions. This is NIO contribution No. 3593.

#### References

- Ngata, Y. (1979): Shallow temperature inversions in the Pacific Ocean near Japan. *J. Oceanogr. Soc. Japan*, 35, 141-150.
- Panakala Rao, D. and J. S. Sastry (1981): Circulation and distribution of some hydrographical properties during the late winter in the bay of Bengal, *Mahasagar. Bull. Nat. Inst. Oceanogr.*, 14, 1-15.
- Prabhakara Rao, B., Ramesh Babu and Chandra Mohan (1987): Seasonal and diurnal variability of thermal structure in the coastal waters off Visakapatnam, *Proc. Indian Acad. Sci. (earth Planet Sci.)*, 96, 69-79.
- Rao, R.R., D. S. Rao, P.G.K. Murthy and M. X. Joseph (1983): A preliminary investigation of the summer monsoonal forcing on the thermal structure of upper Bay of Bengal during Monex-79. *Mausum*, 32, 85-92.
- Fedorov, K. P. (1969) On the vertical stability of temperature inversions in the ocean. *Oceanology*, 9(1), 82-86.
- Shenoi, S.S.C., P.K. Saji and A.M. Almeida, 1999: Near-Surface circulation and kinetic energy in the tropical Indian Ocean derived from Lagrangian drifters, *J. Mar. Res.*, 57, 885-897.
- Shetye, S. R., A. D. Gouveia, D. Shankar, S.S.C. Shenoi, P.N. Vinayachandran, D. Sundar, G.S. Michael, and G. Namboodiri, 1996: Hydrography and circulation in the western bay of Bengal during the northeast monsoon, *J. Geophys. Res.*, 101(6), 14011-14025.
- Suryanarayana, A., V.S.N. Murty and D.P. Rao, 1993: Hydrography and circulation of the Bay of Bengal during early winter, 1983., *Deep. Sea. Res.*, 40(1), 205-217.
- Murty, V.S.N., Y.V.B. Sarma, D.P. Rao and C.S. Murty, 1992: Water characteristics, mixing and circulation in the Bay of Bengal during southwest monsoon, *J. Mar. Res.*, 50, 207-228.
- Darnell, W.L., W.F. Staylor, S.K. Gupta, N.A. Ritchey, and A.C. Wilber, 1992: Seasonal variation of surface radiation budget derived from International Satellite Cloud Climatology Project C1 data. *J. Geophys. Res.*, 97(D14), 15741-15760.